Inorg. Chem. **1985**, *24*, 552–558

infrared spectrum reported by Barrowcliffe et al.[25] Further, formally forbidden modes appear in the infrared spectrum of $Cs_2In^{III}_{0.5}Sb^{V}_{0.5}Cl_6$, but in this case their intensity is independent of temperature.[17] It was postulated that the space group of both compounds is lower than $Fm3m$ and that Cs_2SbCl_6 might undergo a phase change as the temperature is lowered resulting in increased localization of the two Sb valencies in the crystal, in contrast to the mixed-metal In^{III},Sb^{V} salt which shows no evidence of such a transition.

We have found that Cs_2SbCl_6 shows superlattice ordering of $SbCl_6^{3-}$ and $SbCl_6^-$ and the space group is $I4_1/amd$. Sb^{III} and Sb^{V} occupy sites of symmetry D_{2d}, no longer possessing a center of inversion. Taking into account the descent in symmetry from an O_h site to a D_{2d} site, we find that ν_2 and ν_5 should become infrared active. Indeed, ν_2^{V}, ν_5^{V}, and ν_5^{III} are observed in the infrared spectrum of Cs_2SbCl_6. The appearance of ν_1^{V} and ν_1^{III} cannot be explained by using the site-group symmetry properties. Further, ν_3 and ν_4 become Raman active and this might explain the appearance of ν_3^{V} in the resonance Raman spectrum.

In the primitive unit cell of Cs_2SbCl_6, there are two $Sb^{III}Cl_6^{3-}$ and two $Sb^{V}Cl_6^-$ ions, the full factor-group symmetry being D_{4h}, which possesses a center of inversion. The symmetries of the vibrational modes at the zone center involving the $Sb^{III}Cl_6^{3-}$ and $Sb^{V}Cl_6^-$ units can be obtained by the method of ascent in symmetry[27] whereby a representation of a subgroup (i.e. D_{2d}) can be correlated with those representations of the supergroup (i.e. D_{4h}) that are obtained as ascent in symmetry. However, even allowing for the full factor-group symmetry, it is not possible to account for the appearance of ν_1^{III} and ν_1^{V} in the infrared spectrum of Cs_2SbCl_6.

We have also studied the evolution of the structure of $Cs_2M^{III}_{0.5}Sb^{V}_{0.5}Cl_6$ (M = Sb, Bi, Tl) with temperature. No evidence of a phase transition is apparent between 5 and 423 K. The structure is tetragonal at all temperatures, and the only effect present is that of thermal expansion (approximately isotropic). The tetragonal distortion measured by the c/a ratio is effectively constant as are the D_{2d} distortions of the individual $Sb^{V}Cl_6^-$ and $Sb^{III}Cl_6^{3-}$ ions. Hence the change in intensity of the "forbidden" peaks in the infrared spectrum does not seem to arise from a corresponding evolution of the crystal structure. It is worth noticing that similar "forbidden" peaks, though temperature independent, appear in the infrared spectrum of $Cs_2In^{III}_{0.5}Sb^{V}_{0.5}Cl_6$, whose structure is strictly cubic at low temperatures. The $Sb^{V}Cl_6^-$ and $In^{III}Cl_6^{3-}$ ions are constrained by symmetry to be octahedral in this case. Thus it seems more plausible that the origin of these "forbidden" peaks may lie in the involement of vibrational modes away from the Brillouin zone center.[17] Such phonon dispersion may result in the breakdown of the selection rules. Further, the different temperature behavior of the $InCl_6^{3-}$ and $SbCl_6^{3-}$ ions should certainly arise from the different force fields in these ions. Sb^{III} (s^2) contains an "inert" pair of electrons with the result that the forces within the $SbCl_6^{3-}$ ions do not follow the same trends as other MX_6^{n-} units.

Acknowledgment. We thank Dr. A. Hewat, S. Heathman, and Dr. A. Fitch for their help and the Institut Laue-Langevin for providing neutron beam time. K.P. thanks Christ Church, Oxford, for a Senior Scholarship.

Registry No. $Cs_2Sb^{III}_{0.5}Sb^{V}_{0.5}Br_6$, 12397-94-3; $Rb_2Sb^{III}_{0.5}Sb^{V}_{0.5}Br_6$, 36594-17-9; $Cs_2Bi^{III}_{0.5}Sb^{V}_{0.5}Cl_6$, 12441-33-7; $Cs_2Sb^{III}_{0.5}Sb^{V}_{0.5}Cl_6$, 17805-64-0; $Cs_2Tl^{III}_{0.5}Sb^{V}_{0.5}Cl_6$, 41875-61-0; $Cs_2In^{III}_{0.5}Sb^{V}_{0.5}Cl_6$, 41875-60-9; $Cs_2Fe^{III}_{0.5}Sb^{V}_{0.5}Cl_6$, 61269-02-1; $Rb_2Tl^{III}_{0.5}Sb^{V}_{0.5}Cl_6$, 12432-76-7; $Rb_2In^{III}_{0.5}Sb^{V}_{0.5}Cl_6$, 85370-04-3; $Rb_2Fe^{III}_{0.5}Sb^{V}_{0.5}Cl_6$, 61269-01-0; $Rb_2Rh^{III}_{0.5}Sb^{V}_{0.5}Cl_6$, 85370-05-4.

---

(27) Boyle, L. L. *Acta Crystallogr., Sect. A* **1972**, *A28*, 172.

(28) Tovborg-Jensen, A.; Rasmussen, S. E. *Acta Chem. Scand.* **1955**, *9*, 708.

Contribution from the Department of Chemistry and Chemical Physics Program,
Washington State University, Pullman, Washington 99164-4620

Spectroscopic Assignments of the Excited States of *trans*-$(N_2)_2M(Ph_2PCH_2CH_2PPh_2)_2$ (M = W, Mo)

J. G. BRUMMER and G. A. CROSBY*

Received May 14, 1984

Photoluminescence data on the title compound (M = W) in the temperature range of 1.7–300 K have been analyzed in terms of a manifold of emitting levels in thermal equilibrium. A proposed energy level scheme places a $^3B_{1u}$ (W → phosphorus) charge-transfer term lowest followed by a $^3B_{2g}$ ligand field term ~200 cm^{-1} higher in energy. The latter is assumed to be the precursor level(s) for photochemical dissociation of dinitrogen. The orbital scheme (D_{4h}) e_g (d_{xz}, d_{yz}) < b_{2g} (d_{xy}) << a_{2u} (phosphorus d orbitals) < a_{1g} (d_{z^2}) is proposed for the W(0) complex. For the analogous Mo(0) species, the emission data require an inversion of the highest two orbitals placing a_{1g} (d_{z^2}) lower, a scheme that is consistent with the increased photolability of N_2 in the Mo(0) molecule relative to the W(0) analogue.

Introduction

During the past 15 years a number of studies have appeared on the synthesis,[1] thermal reactivity,[2] and photoreactivity[3-5] of *trans*-$(N_2)_2M(dppe)_2$ [M = Mo(0), W(0); dppe = $Ph_2PCH_2CH_2PPh_2$]. Nitrogen dissociation is now known to be

---

(1) (a) George, T. A.; Seibold, C. D. *Inorg. Chem.* **1973**, *12*, 2544. (b) George, T. A.; Seibold, C. D. *J. Organomet. Chem.* **1971**, *C13*, 30. (c) Hidai, M.; Tominari, K.; Uchida, Y.; Misona, A. *Inorg. Synth.* **1974**, *15*, 25. (d) George, T. A.; Noble, M. E. *Inorg. Chem.* **1978**, *17*, 1678. (e) Dilworth, J. R.; Richards, R. L. *Inorg. Synth.* **1980**, *20*, 119.

(2) (a) Chatt, J.; Heath, G. A.; Leigh, G. J. *J. Chem. Soc., Chem. Commun.* **1972**, 444. (b) Chatt, J.; Heath, G. A.; Richards, R. L. *J. Chem. Soc., Dalton Trans.* **1974**, 2074. (c) Chatt, J.; Pearman, A. J.; Richards, R. L.; *Nature (London)* **1975**, *253*, 39. (d) Chatt, J.; Diamantis, A. A.; Heath, G. A.; Hooper, N. E.; Leigh, G. J. *J. Chem. Soc., Dalton Trans.* **1977**, 1688. (e) Colquhoun, H. M. *Acc. Chem. Res.* **1984**, *17*, 23 and references therein.

(3) (a) George, T. A.; Iske, S. D. A. "Proceedings of the First International Symposium on Nitrogen Fixation"; Newton, W. E., Nyman, N. J., Eds.; Washington State University: Pullman, WA, 1976; p 27. (b) Chatt, J.; Diamantis, A. A.; Heath, G. A.; Leigh, G. J.; Richards, R. L. "Proceedings of the First International Symposium on Nitrogen Fixation"; Newton, W. E.; Nyman, N. J., Eds.; Washington State University: Pullman, WA, 1976; p 17. (c) Day, V. W.; George, T. A.; Iske, S. D. A. *J. Am. Chem. Soc.* **1975**, *97*, 4127. (d) Chatt, J.; Pearman, A. J.; Richards, R. L. *J. Chem. Soc., Dalton Trans.* **1977**, 1852. (e) Caruana, A.; Hermann, H.; Kisch, H. *J. Organomet. Chem.* **1980**, *187*, 349.

(4) Chatt, J.; Head, R. A.; Leigh, G. J.; Pickett, J. *J. Chem. Soc., Dalton Trans.* **1978**, 1638.

0020-1669/85/1324-0552$01.50/0

the initial process in photochemical substitution reactions involving these complexes[3e,4] and is believed to occur after initial population of ligand field states of either triplet or singlet character. To relate the photochemistry to the electronic structure, we have embarked on a series of investigations to characterize spectroscopically the lowest lying excited states of the title compounds.

Although spectroscopic studies of both the Mo(0) complex[5] and W(0) species[6] have been reported, no comprehensive model has been proposed to account satisfactorily for the observed properties, largely owing to the lack of experimental data. In this paper we report on the temperature dependence of the emission spectrum and emission lifetime of both bis(diphosphine) compounds in a homogeneous medium. Our aim is to propose orbital and spin designations for their low-lying excited states and to construct a model that satisfactorily accounts for all available spectroscopic evidence and is also in consonance with the photochemistry.

Experimental Section

All solvents used in our synthetic procedures were distilled under nitrogen from the appropriate drying agent. Reactions were also performed under dry nitrogen in Schlenkware vessels. Solution transfers were done by standard Schlenkware methods or inside a glovebox.

$trans$-$(N_2)_2W(dppe)_2$ was prepared according to the published procedure,[1c] with the exception that magnesium metal was replaced by a 0.5% Na/Hg amalgam as the reductant in the final step. Slow diffusion of methanol into a benzene solution of crude product produced bright orange crystals. Anal. Calcd for $(N_2)_2W(dppe)_2$: C, 60.24; H, 4.67; N, 5.40. Found: C, 58.82; H, 4.92; N, 5.20. The infrared spectrum showed the characteristic symmetric and antisymmetric nitrogen stretching frequencies at 2000 cm^{-1} (w) and 1945 cm^{-1} (vs), respectively. Although the elemental analysis indicated an impure product, our 77 K absorption and emission spectra agree well with those reported previously.[6] We did, however, observe a short-lived ($\tau < 100$ ns) impurity emission that we could not eliminate by chemical methods. Previous workers have also observed this emission, and the associated impurity appears to be intrinsic to the synthesis.[7] Since our experimental procedures (vide infra) effectively filtered out this signal, we believe the unidentified impurity produced no insurmountable spectroscopic interference.

$trans$-$(N_2)_2Mo(dppe)_2$ was prepared by the method of George and Seibold.[1a] Pure orange crystals of complex were grown by slow diffusion of methanol into a benzene solution of crude product. Anal. Calcd for $(N_2)_2Mo(dppe)_2$: C, 65.82; H, 5.10; N, 5.91. Found: C, 65.69; H, 5.19; N, 5.70. The infrared spectrum showed the characteristic symmetric and antisymmetric nitrogen stretching frequencies at 2030 cm^{-1} (w) and 1970 cm^{-1} (vs), respectively. Our room-temperature absorption spectrum also agreed with that reported previously.[5]

All absorption and emission spectra were measured on samples dissolved in 2-methyltetrahydrofuran (2-MeTHF). Immediately prior to use, 2-MeTHF was passed over an Al_2O_3 column and then distilled under nitrogen from calcium hydride. We observed no emission of light from the pure solvent at any temperature.

Absorption spectra of samples dissolved in freshly distilled 2-MeTHF at 77 and 298 K were recorded with a Perkin-Elmer Model 330 UV-visible spectrophotometer. For the 298 K measurements the samples were run against a standard 2-MeTHF blank. For the 77 K measurements the glasses were contained in a cylindrical quartz tube of ~2 cm. i.d. mounted in a quartz optical Dewar. Because of shrinkage of the glasses at low temperature, spectra at 77 K vs. air are reported as relative absorbance vs. wavenumber.

Room-temperature infrared spectra were recorded with a Perkin-Elmer 283B spectrometer on solid samples dispersed in KBr. Room-temperature Raman spectra were measured with an ISA Raman spectrometer by utilizing the 6417-Å line of a Lexel Model 85 krypton ion laser. Spectra were obtained from powders of the pure solids as well as concentrated benzene solutions. No compound decomposition was observed. Polarized spectra were recorded from the 9870-Å line of benzene as an internal polarization standard.

Steady-state emission spectra were measured with a spectrometer constructed in the laboratory. A collimated beam of exciting light provided by a 200-W mercury lamp passed through 8 cm of aqueous $CuSO_4$ solution, a Corning 7-60 bandpass filter, and finally a condensing lens before irradiating the sample. The latter, confined in a copper block by an indium O-ring-sealed quartz plate, was mounted in the bore of an Andonian Model 0-24/7 M-H optical Dewar. Temperature was monitored by a calibrated Cryocal carbon glass resistor located near the sample solution; temperatures between 1.7 K and 100 K were attained with this arrangement. Emitted light was collected at right angles to excitation with a lens and then focused with an additional lens through $^1/_2$ in. of aqueous $NaNO_2$ solution onto the slits of a Spex-Minimate monochromator. The dispersed light was detected by a dry ice cooled RCA 7102 photomultiplier tube whose signal was fed to a Keithley Model 610 C electrometer. A PDP 11/23 computer controlled the monochromator through a stepping motor drive. Electrometer output was collected, digitized, and stored by the computer.

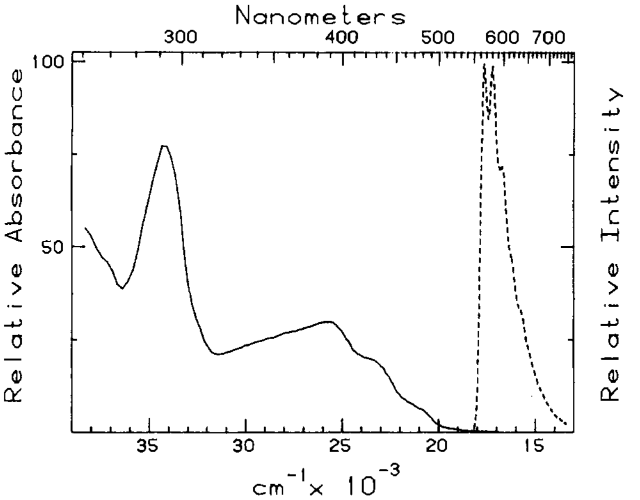

Figure 1. Absorption spectrum (—) and emission spectrum (---) at 77 K of $trans$-$(N_2)_2W(dppe)_2$.

Table I. Absorption Energies for W(0) and Mo(0) Compounds

complex	energy,[a] cm^{-1}	ϵ,[b] $M^{-1}\,cm^2$	complex	energy,[a] cm^{-1}	ϵ,[b] $M^{-1}\,cm^2$
W(0)	20 800	2 000	Mo(0)	23 000	5 900
	23 350	6 300		25 450	11 100
	25 700	11 700		33 300	22 200
	34 150	24 000			

[a] Peak positions at 77 K. [b] Molar extinction coefficient at room temperature (for 77 K peak position).

Time-resolved emission spectra were collected by use of the emission apparatus described above except that a Molectron UV22 nitrogen laser replaced the lamp and the photomultiplier signal was detected with a PAR Model 162 boxcar averager. The latter was triggered by the synchronous output of the nitrogen laser. Delay times from 100 ns to milliseconds could be achieved with this arrangement. All emission spectra were corrected for detection system response and displayed as relative intensity vs. wavenumber.

Excited-state lifetimes were measured via the nitrogen laser; standard right angle geometry was employed. Stray exciting light was filtered out with an aqueous $NaNO_2$ filter. Decay signals were monitored by a fast-wired RCA 7102 photomultiplier tube, displayed on a Tektronix Type 549 storage oscilloscope, photographed, and manually digitized. Plots of ln (intensity) vs. time were linear over at least 2 decay lifetimes, except when noted in the text.

Results and Discussion

The 77 K absorption spectrum of $trans$-$(N_2)_2W(dppe)_2$ in 2-MeTHF is shown in Figure 1. This spectrum is much sharper than that at 298 K and reveals four discernible peaks. The extinction coefficients at the corresponding maxima at room temperature are given in Table I. From the band envelope of the three lowest peaks one might infer that they belong to a single vibrational progression. We discount this possibility since the highest energy band in both the Raman and infrared spectra is the totally symmetric N≡N stretch at ~2000 cm^{-1}, whereas the minimum separation in the electronic spectrum is 2300 cm^{-1}. Thus, we assign all perceptibile bands in the spectrum to distinct electronic origins. Our 77 K absorption spectrum agrees wtih the 143 K spectrum reported by Caruana and Kisch.[6] These authors

---

(5) George, T. A.; Busby, D. C.; Iske, S. D. A. *Adv. Chem. Ser.* **1978**, *No. 168*, 147 and references therein.

(6) Caruana, A.; Kisch, H. *Angew. Chem., Int. Ed. Engl.* **1979**, *18*, 328.

(7) Kisch, H., private communication.

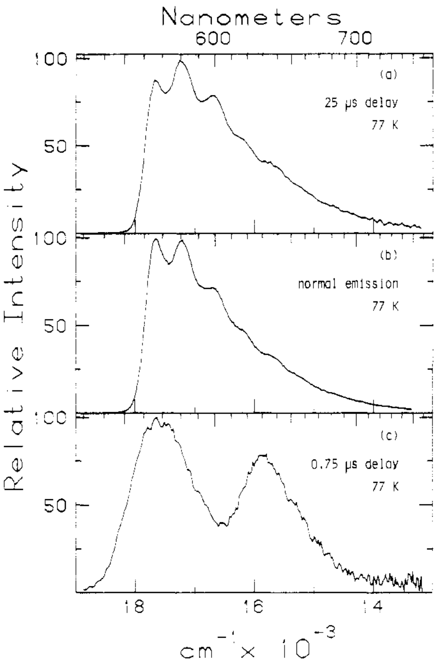

Figure 2. Emission spectra of *trans*-$(N_2)_2W(dppe)_2$ at 77 K: (a) time-resolved spectrum of ~21-μs emission; (b) steady-state spectrum; (c) time-resolved spectrum of <100-ns emission.

also assigned the three lowest absorption bands to separate electronic origins.

Caruana and Kisch first reported the electronic emission (77 K) and excitation (77 K) spectra of *trans*-$(N_2)_2W(dppe)_2$ in 2-MeTHF.[6] We remeasured the 77 K emission spectrum and report it in Figure 1. Our emission spectrum differs from theirs in the relative intensities of the two highest energy peaks (17 700, 17 230 cm^{-1}). In fact, we encountered difficulties reproducing the spectrum of Figure 1 when using alternate samples of complex. Such problems led us to suspect the presence of an emitting impurity. Indeed, Caruana and Kisch now recognize the same impurity emission complicating their spectrum.[7] Because of this experimental complication and our inability to synthesize material of higher purity, we resorted to time-resolved techniques to discriminate against the interfering impurity emission.

Two distinct luminescences of vastly different lifetimes were separated by the boxcar averager. Figure 2a shows the spectrum of the long-lived ($\tau \sim 21$ μs) emission of *trans*-$(N_2)_2W(dppe)_2$ at 77 K. This spectrum was acquired following a 25-μs delay from the synchronous trigger output of the nitrogen laser. Figure 2c shows the spectrum of the short-lived impurity emission ($\tau < 100$ ns) at 77 K, which was recorded following a 0.75-μs delay from the excitation pulse. A 50-ns sampling window was used to record Figure 2a,c. Comparison of spectra in Figure 2a,c with the steady-state emission spectrum (77 K) shown in Figure 2b eliminates the inconsistency of the relative intensities of the two highest energy emission bands. Fortuitously, the high-energy peaks of both the long-lived and short-lived emission spectra maximize at approximately the same energy. The normal emission spectrum (Figure 2b) is a weighted superposition of the spectra shown in Figure 2a,c.

Time resolution techniques also allowed us to probe the temperature dependence of the emission spectrum of the W(0) compound. The results are displayed in Figure 3 for temperatures of 8, 65, and 80 K. All three spectra were recorded after a 25-μs delay from the laser pulse and with a sampling window of 50 ns, effectively eliminating any impurity light. Since no variation in the spectral band shape with temperature occurred below 30 K, we conclude that the emission spectrum arises from a single electronic state in this temperature domain. The 8 K spectrum, maximizing at 17 720 cm^{-1}, is shown in Figure 3c. As the temperature was raised, the emission intensity decreased and the spectral band shape changed. The 80 K spectrum is shown in Figure 3a. It maximizes at 17 250 cm^{-1}. We infer from the foregoing evidence that a new weak-emission band is growing in with increasing temperature, at the expense of the dominant intense low-temperature component. Such behavior is indicative of a manifold of emitting levels whose relative populations are governed by the temperature.

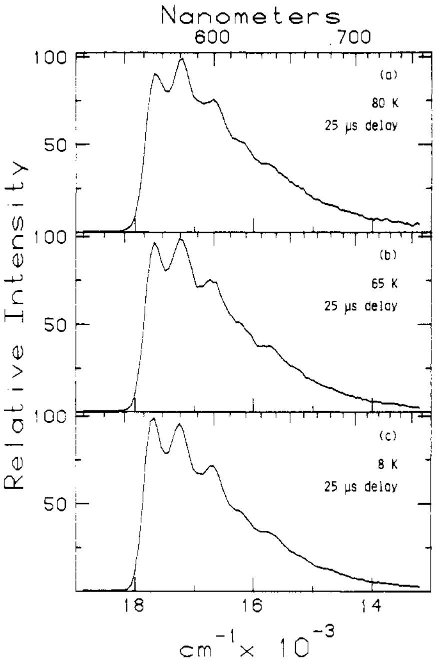

Figure 3. Time-resolved emission spectra of *trans*-$(N_2)_2W(dppe)_2$ as a function of temperature: (a) 80 K; (b) 65 K; (c) 8 K.

Table II. Emission Energies for W(0) and Mo(0) Compounds

complex	energy, cm^{-1}	ΔE, cm^{-1}	τ, μs
trans-$(N_2)_2W(dppe)_2$[a]	17 720[b]		21 (77 K), 24 (14 K)
	17 250	470	
	16 720	530	
	16 250	470	
	15 750	500	
	15 250	500	
	14 750	500	
trans-$(N_2)_2Mo(dppe)_2$[c]	15 700[b]		28 (14 K)

[a] Peak energies for 8 K spectrum. [b] Spectral maximum. [c] Peak energy for 10 K spectrum.

The 8 K emission spectrum (Figure 3c) shows seven peaks separated by approximately 500 ± 30 cm^{-1}. The peak energies are given in Table II. The solid-state Raman spectrum reveals a band at 525 ± 3 cm^{-1}. Polarized Raman experiments on benzene solutions show this band to be totally symmetric. From the regular peak spacings in emission and the near-coincident vibrational resonance in the Raman spectrum, we conclude that the structure in the 8 K emission spectrum is entirely vibronic in origin. The most intense peak of the progression lies at 17 720 cm^{-1} and is assigned to the origin of a Franck–Condon-allowed transition. Since no mirror image band appears in the 77 K absorption spectrum, we infer that the lowest energy absorption band has a different electronic origin than the prominent emission band.

The 80 K emission spectrum of *trans*-$(N_2)_2W(dppe)_2$ is shown in Figure 3a. Its maximum is red-shifted from the 8 K spectral (Figure 3c) maximum, consistent with a new emitting state gaining population at higher temperature. Caruana and Kisch report an emission quantum yield of 0.08 at 77 K.[6] From the similarity of the time-resolved and steady-state emission spectra at this same temperature (Figure 2a,b, respectively), we feel that 0.08 is still a reasonable number. As the temperature is lowered toward 8 K, the intensity of the peak at 17 720 cm^{-1} increases by a factor of ~2. If we take this peak height to be a reasonable measure

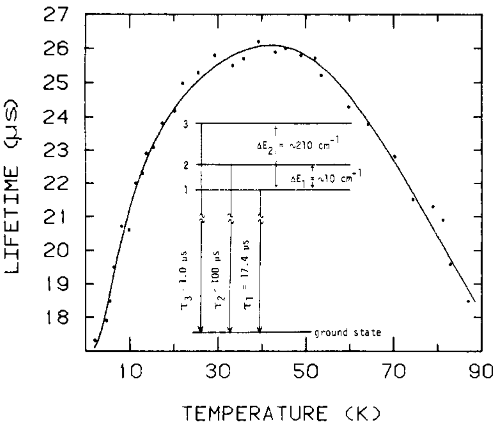

Figure 4. Emission lifetime as a function of temperature for *trans*-$(N_2)_2W(dppe)_2$. Inset gives results of fitting lifetime vs. temperature data to eq 1.

of peak area, we conclude that the state primarily responsible for the emission spectrum at 8 K has a quantum yield of ca. 0.16. The upper emitting state, i.e., the one giving rise to the spectral shift upon increasing temperature, must possess a quantum yield that is significantly less than 0.08.

An equilibrium manifold of excited states is also implied by the invariance of the spectral band shape with delay time (>25 μs) at any given temperature as recorded on the boxcar averager. Switching the delay time from 25 to 50 μs produced no band-shape changes in the emission spectra of Figure 3. If the overall emission spectrum arose from a superposition of spectra from two nonequilibrated states with different lifetimes, changes in delay time would certainly lead to changes in spectral band shape. Only in the improbable circumstance of two emitting states possessing identical spectra would the band shape remain invariant. This is clearly not the case for *trans*-$(N_2)_2W(dppe)_2$. We conclude that the levels responsible for the observed emission spectrum are thermally equilibrated within the microsecond time domain.

The emission lifetime of *trans*-$(N_2)_2W(dppe)_2$ at 77 K is 21 μs. This value is in reasonable agreement with the 19-μs lifetime previously reported by Caruana and Kisch.[6] As shown in Figure 4 the lifetime is temperature dependent between 2 and 90 K, and above 90 K plots of ln (intensity) vs. time are nonlinear.

The 77 K absorption spectrum of *trans*-$(N_2)_2Mo(dppe)_2$ in 2-MeTHF is shown in Figure 5. This spectrum has much more structure than the envelope at 298 K and reveals three distinct bands. The extinction coefficients of the corresponding peaks in the 298 K spectrum are given in Table I. By analogy to *trans*-$(N_2)_2W(dppe)_2$ we assign the absorption bands to separate electronic transitions. George et al.[5] reported the 298 K absorption spectrum of the Mo(0) complex in benzene solution. Our 298 K spectrum agrees with their previously published result. These authors also assigned the absorption peaks to distinct electronic transitions.

trans-$(N_2)_2Mo(dppe)_2$ displayed a weak peach-colored emission at 77 K. Although we measured no emission quantum yield for the complex, a conservative estimate places it at least a factor of 5 below that taken at 10 K of the analogous W(0) compound. As the temperature of the molybdenum species was lowered below 77 K, the emission became more intense. The 10 K steady-state emission spectrum is displayed in Figure 5. The spectrum maximizes at 15 700 cm^{-1}. Between 2 and 77 K we detected no band-shape changes. In contrast to *trans*-$(N_2)_2W(dppe)_2$ the emission spectrum of the Mo(0) compound is broad and is unstructured at all temperatures. To our knowledge we are the first to report an emission from this complex.

Emission decays of the Mo(0) complex yielded nonlinear plots of ln (intensity) vs. time at nearly every temperature. Such behavior precluded the application of a lifetime vs. temperature analysis such as the one applied to the W(0) species. We did obtain linear plots near 14 K, however, and report an emission lifetime of 28 μs at this temperature.

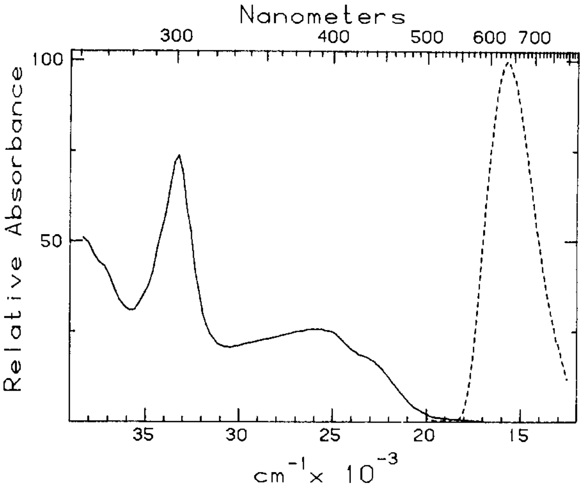

Figure 5. Absorption spectrum (—) at 77 K and emission spectrum (---) at 10 K of *trans*-$(N_2)_2Mo(dppe)_2$.

Data Reduction Methods. Our method of data analysis, which has been developed previously,[8] assumes an emitting manifold of thermally equilibrated states. The equation appropriate for describing the measured lifetime, $\tau(T)$, of this system is given by

$$\tau(T) = \frac{1 + \exp(-\Delta E_1/kT) + \exp(-\Delta E_2/kT)}{k_1 + k_2 \exp(-\Delta E_1/kT) + k_3 \exp(-\Delta E_2/kT)} \quad (1)$$

where ΔE_1 and ΔE_2 are the energy gaps between levels 1 and 2 and levels 1 and 3, respectively, and k_1–k_3 are the total rate constants for deppopulating levels 1–3 directly to the ground state. No degeneracy factors were included during our analysis of the data, although our proposed model (vide infra) indicates that the lower level is doubly degenerate. The physical assumptions implicit in the above equation are (a) each level in the emitting manifold decays to the ground state by first-order processes with temperature-independent radiative and nonradiative rate constants and (b) equilibrium is established among the levels in times much shorter than the lifetime of the decaying manifold.

The temperature-dependent lifetime data were analyzed with a multiparameter least-squares curve-fitting computer program[9] to attain the five constants ΔE_1, ΔE_2, and k_1–k_3 contained in eq 1 and included in Figure 4. We emphasize that three levels are all that are needed to fit the experimental data. We also stress that, at all temperatures below 90 K, plots of ln (intensity) vs. time were linear over at least 2 lifetimes. This behavior supports the assumptions underlying our analysis.

Spin and Configurational Assignments. Uchida et al. have published the crystal structure of *trans*-$(N_2)_2Mo(dppe)_2$.[10] Molybdenum occupies the center of symmetry of the molecule and is coplanar with the four ligating phosphorus atoms. The two dinitrogen molecules are trans; however, the N≡N—Mo—N≡N linkage is not linear. The local symmetry about the central molybdenum is D_{4h}; moreover, phosphorus-31 NMR data[1a] show that this configuration is retained in homogeneous solution. From the correspondence of their infrared and electronic absorption spectra, and in the absence of evidence to the contrary, we infer that the W(0) complex has symmetry identical with that of the Mo(0) complex.

Crosby has recently discussed the criteria for assigning electronic states of high-microsymmetry, d^6 transition-metal complexes.[11] These criteria are based on a large body of experimental fact and theoretical argument. We will use these criteria, as well as those developed by other workers for high-symmetry transition-metal complexes,[12] to guide us in assigning the excited states responsible

---

(8) Hager, G. D.; Crosby, G. A. *J. Am. Chem. Soc.* **1975**, *97*, 7031.

(9) Bevington, P. R.; "Data Reduction and Error Analysis for the Physical Sciences"; McGraw-Hill: New York, 1969.

(10) Uchida, T.; Uchida, Y.; Hidai, M.; Kodama, T. *Acta Crystallogr., Sect. B: Struct. Crystallogr. Cryst. Chem.* **1975**, *B31*, 1197.

(11) Crosby, G. A. *J. Chem. Educ.* **1983**, *60*, 791.

for the absorption and emission spectra of the title compounds.

Absorption Spectra. The 77 K absorption spectrum of *trans*-$(N_2)_2Mo(dppe)_2$ shows three definite peaks. The corresponding bands in the 298 K spectrum all have extinction coefficients of 5900 M^{-1} cm^2 or greater as shown in Table I. The magnitudes of these extinctions are larger than those expected for metal–centered d–d transitions, especially for complexes of such high symmetry. Moreover, the spin–orbit coupling constant[13] for Mo(0) is only ~552 cm^{-1} and is probably too small to allow spin-forbidden transitions to appear in absorption, especially with an extinction larger than 5900 M^{-1} cm^2. We, therefore, attribute these bands to singlet–singlet, metal-to-ligand charge-transfer (MLCT) transitions.

Further support for this view comes from the absorption spectrum of the Mo(0) complex measured by George et al.[5] They showed the two low-energy absorption bands to be sensitive to the nature of the diphosphine ligand. For example, replacing phenyl by ethyl on the ligating phosphorus atom shifted these two absorption bands to higher frequencies. Such behavior is consistent with the greater electron-donating ability of the ethyl group if the bands correspond to MLCT excited states involving the phosphorus atom. Shifting the energies of the first two absorption bands in the ethyl-substituted compound to higher frequencies also uncovered two more weak absorption bands at 20 580 cm^{-1} (ϵ = 590 M^{-1} cm^2) and 21 980 cm^{-1} (ϵ = 590 M^{-1} cm^2). From a consideration of their extinction coefficients, George et al. assigned these bands to ligand field (LF) transitions. Unfortunately, the absorption data on the two Mo(0) complexes were taken in two different solvent systems, causing some uncertainty concerning the correspondence of bands. We are currently investigating the ethyl-substituted compound in order to clarify the spectra.

In summary, we assign the two lowest energy absorption bands of *trans*-$(N_2)_2Mo(dppe)_2$ to spin-allowed MLCT transitions involving significant phosphorus atom contribution. These bands may be obscuring two weak spin-allowed LF transitions apparent in the absorption spectrum of the analogous ethyl-substituted complex. The origin of the strong absorption band at 33 000 cm^{-1} is still unknown, although the π^* orbitals on N_2 may be involved. We are continuing our investigation of these absorption spectra.

In contrast to the Mo(0) complex, *trans*-$(N_2)_2W(dppe)_2$ shows four distinct absorption peaks (Figure 1). The three highest energy bands at 23 350, 25 700, and 34 150 cm^{-1} nearly coincide with the three absorption bands of *trans*-$(N_2)_2Mo(dppe)_2$ in both energy and intensity (Table I). In the absence of any substituent studies on the W(0) compound we assign the absorption bands at 23 350 and 25 700 cm^{-1} to spin-allowed MLCT transitions by analogy to the Mo(0) case. The 20 800-cm^{-1} band unique to *trans*-$(N_2)_2W(dppe)_2$ has an extinction coefficient of ~2000 M^{-1} cm^2. Such a low intensity raises the possibility of this band possessing spin-forbidden character, especially in light of the large spin–orbit coupling constant for W(0) ($\zeta_{W(0)}$ = 2089 cm^{-1}).[13] However, the lowest energy emission band (Figure 3c) and the first absorption band do not possess mirror symmetry. Thus, our assignment of the emission to a MLCT spin-forbidden transition (vide infra) renders improbable a singlet → triplet (MLCT) assignment for the low-energy absorption band. A LF assignment for this weak band is also rejected on the basis of simple crystal field arguments, since, progressing down a column of the periodic table one expects values of 10*Dq* to increase and to shift the LF transitions in *trans*-$(N_2)_2W(dppe)_2$ to higher energies than those in the corresponding Mo(0) complex. In fact, the LF transitions should be obscured by the three intense MLCT transitions. Thus, we assign this absorption band at 20 800 cm^{-1} to a spin-allowed MLCT transition also. The insensitivity of the energy of the MLCT absorption bands to the identity of the central metal is puzzling, and we offer no explanations for it.

Emission Spectra. Our emission data, temperature-dependent emission spectra, temperature-dependent lifetimes, and the evident invariance of the emission spectrum with boxcar delay time support the model of a thermally equilibrated manifold of emitting states for *trans*-$(N_2)_2W(dppe)_2$. A fit of the lifetime vs. temperature data implies a manifold consisting of three states spanning ~210 cm^{-1}. The energy gaps between states (ΔE_i) and overall rate constants ($k_i = k_i^r + k_i^{nr}$) for depopulating each state are contained in Figure 4. From the temperature dependence of the emission spectrum we infer both the first and third states of the manifold to have significant radiative character. Furthermore, our observations of emission intensity vs. temperature place the quantum yield of the lowest state much higher than that of the uppermost one. From the constancy of the spectral band shape between 2 and ~30 K and the rate constants obtained from a fit of the lifetime data to eq 1 we conclude that the middle state in the three-state manifold is virtually nonradiative.

The lowest excited state of the complex produces the highly structured emission spectrum reproduced in Figure 3c. The 500 ± 30 cm^{-1} vibrational spacing in this emission, the totally symmetric band at 525 ± 3 cm^{-1} in the Raman spectrum, and the substantial emission quantum yield (~0.16) point toward a symmetry-allowed transition. The prominent vibronic progression evident on the electronic envelope, the correspondence with an A_{1g} frequency in the Raman spectrum, and the obvious Franck–Condon-allowed nature of the band envelope lead us to assign the peak at 17 720 cm^{-1} to the electronic origin of the transition. That the electronic origin is the most intense member of the vibronic progression indicates little distortion between the ground- and excited-state potential wells. Whether the totally symmetric vibration seen in emission involves the W–N or W–P stretching motion is a question currently under investigation. We favor the latter option (vide infra). From these spectral attributes, the significant emission quantum yield, and the measured decay time of ~17 μs we assign the lowest emissive excited state of *trans*-$(N_2)_2W(dppe)_2$ to an allowed MLCT state involving a substantial degree of triplet character.

The unresolved band growing into the emission spectrum at high temperatures (30–90 K) is red-shifted from the 17 720-cm^{-1} low-temperature origin. Reasoning in terms of a simple thermally equilibrated manifold of emitting states, one would expect the high-temperature band to be shifted to higher, not lower, energies. Our conclusion is that the electronic transition responsible for the high-temperature band is accompanied by considerable geometrical distortion. In d^6 D_{4h} complexes such as *trans*-$(N_2)_2W(dppe)_2$ LF transitions are orbitally forbidden, involving promotion of an electron from a metal-localized nonbonding orbital to a σ-antibonding orbital with respect to metal–ligand interaction. Such transitions should be accompanied by significant geometrical distortion and low levels of emitted light. Hipps, Merrell, and Crosby investigated the geometrical distortion accompanying LF transitions in some d^6 complexes of O and D_4 symmetry.[14] All spectra showed prominent vibrational progressions that maximized at the seventh or eighth member removed from the electronic origin. These authors also determined bond length changes as large as 0.16 Å by subjecting the emission bands to Franck–Condon analyses. Because of the low-emission quantum yield, the inferred large geometrical distortion, and the 1.0-μs emission lifetime, we assign the highest energy emitting component of the manifold to a LF state of triplet character.

The emission behavior of *trans*-$(N_2)_2Mo(dppe)_2$ contrasts sharply with that of the W(0) complex. The spectrum at 77 K is shown in Figure 5. It is broad and structureless; moreover, the intensity is low. We estimate the quantum yield to be at least a factor of 5 less than that of the W(0) compound. From the long emission lifetime (28 μs at 14 K) coupled with the low-emission quantum yield we infer that the radiative life is on the order of milliseconds. This intrinsically long life and the structureless emission spectrum point to a predominantly spin-forbidden LF assignment for the dominant emitting state of this complex. Further justification for this assignment derives from the two

---

(12) Gray, H. B.; Ballhausen, C. J. *J. Am. Chem. Soc.* **1963**, *85*, 260.

(13) Griffiths, J. S. "The Theory of Transition Metal Ions"; Cambridge University Press: London, 1964; p 113.

(14) Hipps, K. W.; Merrell, G. A.; Crosby, G. A. *J. Phys. Chem.* **1976**, *80*, 2232.

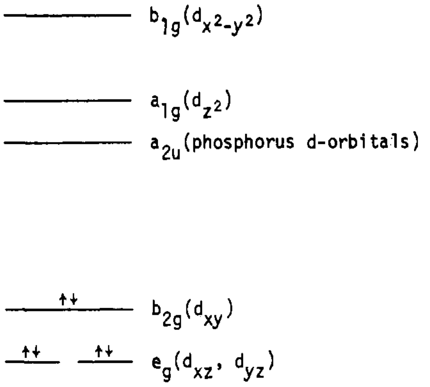

Figure 6. Proposed molecular orbital ordering for *trans*-$(N_2)_2W(dppe)_2$ in D_{4h} symmetry. Ordering of d_{z^2} and a_{2u} orbitals is inverted for *trans*-$(N_2)_2Mo(dppe)_2$.

low-energy absorption bands exhibited by *trans*-$(N_2)_2Mo(depe)_2$ where depe = $Et_2PCH_2CH_2PEt_2$.[5] These weak bands ($\epsilon \sim 590$ M^{-1} cm^2) may correspond to the spin-allowed counterpart of the LF emission of *trans*-$(N_2)_2Mo(dppe)_2$.

Orbital and State Assignments. To rationalize our assignments we propose the simple (D_{4h}) molecular orbital scheme depicted in Figure 6. The orbital ordering essentially agrees with that proposed by Gray and Ballhausen for square-planar complexes.[12] In our view the axial dinitrogens cause the d_{z^2} orbital to rise in energy above the d_{xy}, consistent with the tetragonal distortion pattern expected for axial ligation, even for weak-field axial ligands. Our experimental results (vide infra) necessitate placing the phosphorus acceptor π orbital of a_{2u} symmetry lowest among unoccupied molecular orbitals. This proposed molecular orbital ordering differs from that used by other workers to explain the spectroscopy of d^8 square-planar $[Ir^I(2{=}phos)_2]^+$,[15] $[Rh^I(2{=}phos)_2]^+$,[15] $[Pd^{II}(CN)_4]^{2-}$,[16] and $[Pt^{II}(CN)_4]^{2-}$.[16] These authors have adopted an occupied molecular orbital ordering of $d_{xy} < d_{xz}$, $d_{yz} < d_{z^2} < d_{x^2-y^2}$. This alternate ordering was also used by George et al. to explain the absorption behavior and photochemistry of *trans*-$(N_2)_2Mo(dppe)_2$.[5] Our experimental results, however, point to the orbital ordering given in Figure 6.

According to this model the three lowest energy spin-allowed absorption bands expected for *trans*-$(N_2)_2M(dppe)_2$ [M = Mo(0), W(0)], consistent with a MLCT assignment, are b_{2g} (d_{xy}) $\rightarrow$ a_{2u}, e_g (d_{xz}, d_{yz}) $\rightarrow$ a_{2u}. These promotions produce excited states of symmetry $^1B_{1u}$ and ^1E_u, respectively (see Figure 7). The crystal structure of the Mo(0) compound indicates that the local symmetry about the central metal may be distorted toward D_{2h}, in which case ^1E_u would split into two nondegenerate states. Transitions from the $^1A_{1g}$ ground state to ^1E_u (D_{4h}) are allowed by symmetry and should lead to absorption bands of reasonable intensity. We assign the absorption bands at 23 350 cm^{-1} (ϵ = 6300 M^{-1} cm^2), 25 700 cm^{-1} (ϵ = 11 700 M^{-1} cm^2) and 23 000 cm^{-1} (ϵ = 5900 M^{-1} cm^2), 25 450 cm^{-1} (ϵ = 11 100 M^{-1} cm^2) to the split components of $^1A_{1g} \rightarrow {}^1E_u$ (D_{4h}) of the W(0) and Mo(0) complexes, respectively. Transitions to $^1B_{1u}$ are symmetry forbidden and become allowed only through a vibronic mechanism. The $^1A_{1g} \rightarrow {}^1B_{1u}$ transition should therefore be weak, if present at all. We assign it to the peak at 20 800 cm^{-1} ($\epsilon \sim 2000$ M^{-1} cm^2) in the W(0) complex and believe it too weak to be seen in the Mo(0) complex. Any absorption bands of ligand field parentage are probably obscured by the more allowed charge-transfer transitions.

Our assignment of the low-temperature emission spectrum of *trans*-$(N_2)_2W(dppe)_2$ (Figure 3c) to a spin-forbidden MLCT excited state is also consistent with the proposed model. The triplet term arising from the b_{2g} (d_{xy}) $\rightarrow$ a_{2u} orbital promotion is $^3B_{1u}$.

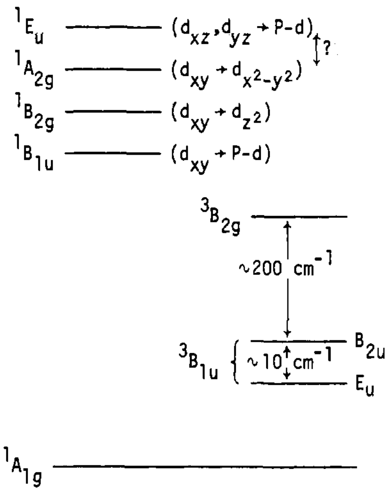

Figure 7. Proposed symmetry assignments for lowest lying excited terms of *trans*-$(N_2)_2W(dppe)_2$ in D_{4h} symmetry. Ordering of B_{2g} and B_{1u} terms are inverted for *trans*-$(N_2)_2Mo(dppe)_2$.

In the D_4 double group $^3B_{1u}$ splits into two states, a nondegenerate B_{2u} and a degenerate E_u component. The E_u state is formally allowed and could gain intensity by mixing with higher ^1E_u states under spin-orbit coupling. The B_{2u} state is formally forbidden. We identify the latter with the essentially nonradiative state lying $\sim$10 cm^{-1} above the lowest E_u component in the excited manifold. The existence of an essentially nonradiative state is required to fit the lifetime vs. temperature data.

The diffuse band growing into the emission spectrum of *trans*-$(N_2)_2W(dppe)_2$ at higher temperatures (30–90 K) is assigned to a spin-forbidden LF transition. The lowest energy LF promotion in Figure 7 is b_{2g} (d_{xy}) $\rightarrow$ a_{1g} (d_{z^2}) and leads to excited terms of $^1B_{2g}$ and $^3B_{2g}$ symmetry. The fact that the $^3B_{2g} \rightarrow {}^1A_{1g}$ transition is both orbitally and spin forbidden would account for its much lower emission intensity compared to that of the $^3B_{1u} \rightarrow {}^1A_{1g}$ MLCT transition. The temperature-dependent lifetime data place a highly distorted state $\sim$210 cm^{-1} above the $^3B_{1u}$ term. We identify this state with the $^3B_{2g}$ LF term.

From its spectral characteristics the only emission observed from *trans*-$(N_2)_2Mo(dppe)_2$ appears to be LF in origin. In addition, the absorption spectrum of *trans*-$(N_2)_2Mo(depe)_2$ reveals two low-energy low-extinction bands that may also be LF in nature. From this evidence we conclude that the a_{1g} (d_{z^2}) molecular orbital lies below the a_{2u} phosphorus acceptor orbital in the Mo(0) compounds in contradistinction to the tungsten analogue. Consequently, only the $^3B_{2g} \rightarrow {}^1A_{1g}$ transition is observed in emission for *trans*-$(N_2)_2Mo(dppe)_2$.

Conclusions

Our assignments for the lowest excited states of the title compounds are summarized in Figure 7. The lowest energy absorption band in the W(0) complex involves excitation to a MLCT $^1B_{1u}$ term. Emission emanates from an equilibrated manifold of three states. The lowest two states of the manifold arise from a MLCT $^3B_{1u}$ term, which, under the influence of spin-orbit coupling, splits into a B_{2u} state and a degenerate E_u level. The E_u level is formally allowed, lies lowest in energy, and gives rise to the structured low-temperature emission of Figure 3c. The B_{2u} state lies 10 cm^{-1} higher and is essentially nonradiative. The band growing into the emission spectrum at high temperature arises from a $^3B_{2g}$ term of LF parentage. In the Mo(0) complex, the $^3B_{2g}$ term drops below the MLCT $^3B_{1u}$ term and only a weak broad unstructured emission is observed. Evidence for the $^1A_{1g} \rightarrow {}^1B_{2g}$ transition lying lowest in absorption has been provided by George et al.[5]

That the $^1B_{2g}$ and $^3B_{2g}$ terms are the lowest lying excited levels of *trans*-$(N_2)_2Mo(dppe)_2$ is consistent with the dissociative photochemistry observed for this complex. The b_{2g} (d_{xy}) $\rightarrow$ a_{1g} (d_{z^2}) orbital promotion responsible for the transitions involves excitation from an essentially nonbonding orbital on Mo(0) to a σ-antibonding orbital with respect to metal–nitrogen interaction. This

---

(15) (a) Geoffroy, G. L.; Wrighton, M. S.; Hammond, G. S.; Gray, H. B. *J. Am. Chem. Soc.* **1974**, *96*, 3105. (b) Fordyce, W. A.; Crosby, G. A. *Inorg. Chem.* **1982**, *21*, 1455.

(16) Piepho, S. B.; Schatz, P. N.; McCaffery, A. J. *J. Am. Chem. Soc.* **1969**, *91*, 5994.

excitation should therefore lead to a weakening of the metal-nitrogen bond and ultimate dinitrogen dissociation. In the W(0) complex the $^1B_{1u}$ and $^3B_{1u}$ MLCT terms lie lower in energy than the LF terms. Excitation of MLCT states is not expected to lead to dissociative photochemistry; however, ~200 cm^{-1} higher than the $^3B_{1u}$ term lies the $^3B_{2g}$ LF term. This potentially dissociative state can be populated thermally even at low temperatures. One would therefore expect a temperature dependence of N_2 dissociation for the W(0) complex. No such dependence is predicted for the Mo(0) compound. Even at room temperature, the greater population of the $^3B_{2g}$ term in *trans*-$(N_2)_2$Mo(dppe)$_2$ as opposed to *trans*-$(N_2)_2$W(dppe)$_2$ should lead to a greater photoreactivity for the former complex. This inference, derived entirely from spectroscopic evidence, agrees with the known relative photoreactivities of the two molecules.[4]

Acknowledgment. This research was supported by the National Science Foundation (Grant No. CHE-8119060).

Registry No. *trans*-$(N_2)_2$W(dppe)$_2$, 28915-54-0; *trans*-$(N_2)_2$Mo(dppe)$_2$, 25145-64-6.

Contribution from the Istituto Teoria, Struttura Elettronica Composti di Coordinazione del CNR, Area di Ricerca di Roma, Rome, Italy, and Inorganic Chemistry Laboratory, Oxford University, Oxford OX1 3QR, England

Low-Temperature Optical and Magneto-Optical Study of the Organic-Intercalated Two-Dimensional Ferromagnet $(CH_3NH_3)_2CrCl_4$

CARLO BELLITTO, TERENCE E. WOOD, and PETER DAY*

Received June 5, 1984

Optical absorption spectra have been measured of single crystals of the two-dimensional ferromagnet $(CH_3NH_3)_2CrCl_4$ in the region of the quintet-to-triplet ligand field transitions at 5330 and 6270 Å at temperatures from 1.6 to 9 K and magnetic fields up to 5 T applied parallel to [010] of the *Aba*2 unit cell. Above 2 K the absorption is dominated by "hot" exciton–magnon combinations, but at the lowest temperatures there is evidence for cold-band intensity arising from a small amount of spin canting, as in Rb_2CrCl_4. Quantitative analysis of the temperature and field dependence of the intensity and line shape of the bands gives an estimate of the anisotropy gap in the magnon spectrum at the Brillouin zone center as 1.9 (3) K and g = 1.93 (1).

Introduction

Very few ionic transition-metal compounds order ferromagnetically, and among this small group even fewer have resolved ligand field transitions that permit quantitative studies of the optical and magneto-optical properties. In this respect the tetrahalogenochromate(II) salts are probably unique because they have two groups of sharp bands arising from quintet-to-triplet transitions, which constitute the only visible absorption.[1] The behavior of these bands as a function of temperature and applied field has been studied in detail in Rb_2CrCl_4,[2] which has a structure related to the K_2NiF_4 structure, but with a cooperative Jahn–Teller distortion around the high-spin 3d^4 cations within the basal plane.[3]

As well as the group 1[24] tetrachlorochromates(II), there also exists a series of organic-intercalated salts $(RNH_3)_2CrCl_4$[4] (R = C_nH_{2n+1}; n = 1–12) that are quite similar to the layer perovskite halide salts of Mn(II), Fe(II), Cu(II), and Cd(II), whose magnetic properties and structural phase transitions have been widely studied.[5,6] We reported susceptibility and magnetization data on n = 1, 2, 3, 5, and 12 examples[7,8] and the variation of the visible absorption bands in the C_1 and C_2 compounds from about 10 to 150 K.[7] In these ferromagnets, as in the prototype Rb_2CrCl_4, the electric dipole intensity of the formally spin-forbidden transitions arises from combining the creation of an exciton, $\epsilon(k)$, which lowers the total spin projection of the crystal, with annihilation of a thermally populated spin fluctuation (magnon) $m(-k)$. The combined process $\epsilon(k) - m(-k)$ conserves momentum and is thus brought about by photon absorption for all values of k, i.e. across the whole Brillouin zone. The band shape is therefore determined by convoluting the exciton and magnon densities of states and the intensity at a given temperature by the Bose population of magnons. For a square-planar two-dimensional Heisenberg ferromagnet with negligible anisotropy, an intensity proportional to T^2 was predicted[9] and found above 10 K in the Rb,[10] C_1, and C_2 salts.[7] However, since the ground state has S = 2, anisotropy cannot be neglected, and at temperatures where kT becomes comparable to the anisotropy energy, the T^2 law should fail. In Rb_2CrCl_4 this occurs below 4 K[2,11] so in the present paper we report absorption spectra of $(CH_3NH_3)_2CrCl_4$ from 1.6 to 9 K and extract an estimate of the zone-center anisotropy gap in the magnon density of states for comparison with that of the Rb salt. The zone-center gap can also be varied by applying a field,[11] and the variation in absorption band intensities from 0 to 5 T is also reported. Finally, if there is any canting of the moments from collinearity, it is predicted[12] that the small antiferromagnetic component should lead to a cold-band contribution to the intensity which, however, may be masked by the greater hot-band intensity, except at very low temperatures.

Experimental Section

$(CH_3NH_3)_2CrCl_4$ crystals used for this work were prepared as reported previously.[7] They are extremely air-sensitive, and all solvents etc. must be rigorously oxygen free. All manipulations were carried out by Schlenk techniques under O_2-free nitrogen. Methylammonium chloride was from BDH, and the starting solution of Cr(II) in ethanol was obtained by dissolving electrolytic Cr metal with HCl gas. Good crystals for optical measurements were obtained by a slow cooling of a saturated ethanolic solution of the title compound sealed in a heavily walled ampule. Typically, for 0.5 g of the compound 15 mL of absolute ethanol is needed for solution. Crystal faces were identified easily because the compound crystallizes as platelets, the main face being [010] of the orthorhombic space group *Aba*2.

Absorption spectra were recorded on either a Cary 14 spectrophotometer or a McPherson double-beam spectrophotometer. Temperatures between room temperature and 77 K were recorded with an Oxford Instrument CF 100 cryostat. Spectra below liquid-nitrogen temperature

---

* To whom correspondence should be addressed at Oxford University.

(1) For a review, see: Day, P. *Acc. Chem. Res.* **1979**, *12*, 236.
(2) Janke, E.; Wood, T. E.; Ironside, C.; Day, P. *J. Phys. C* **1982**, *15*, 3809.
(3) Day, P.; Hutchings, M. T.; Janke, E.; Walker, P. J. *J. Chem. Soc., Chem. Commun.* **1979**, 711. Janke, E.; Hutchings, M. T.; Day, P.; Walker, P. J. *J. Phys. C* **1983**, 16, 5959.
(4) Bellitto, C.; Day, P. *J. Chem. Soc., Chem. Commun.* **1976**, 870.
(5) de Jongh, L. J.; Miedema, A. *Adv. Phys.* **1974**, *24*, 1.
(6) Blinc, R.; Zeks, B.; Kind, R. *Phys. Rev. B: Solid State* **1978**, *17*, 3049.
(7) Bellitto, C; Day, P. *J. Chem. Soc., Dalton Trans.* **1978**, 1207.
(8) Stead, M. J.; Day, P. *J. Chem. Soc., Dalton Trans.* **1982**, 1081.
(9) Gregson, A. K.; Day, P.; Okiji, A.; Elliott, R. J. *J. Phys. C* **1976**, *9*, 2481.
(10) Day, P. *Colloq. Int. CNRS* **1976**, 255, 237.
(11) Day, P.; Janke, E.; Wood, T. E.; Woodwark, D. *J. Phys. C* **1979**, *12*, L329.
(12) Elliott, R. J.; Hengeltraub, A.; Harrop, M. C.; Ziman, T. A. L. *J. Magn. Magn. Mater.* **1980**, *15–18*, 359.

0020-1669/85/1324-0558$01.50/0